

This article was downloaded by:

On: 24 January 2011

Access details: *Access Details: Free Access*

Publisher *Taylor & Francis*

Informa Ltd Registered in England and Wales Registered Number: 1072954 Registered office: Mortimer House, 37-41 Mortimer Street, London W1T 3JH, UK



Journal of Macromolecular Science, Part A

Publication details, including instructions for authors and subscription information:

<http://www.informaworld.com/smpp/title~content=t713597274>

Semibatch Emulsion Polymerization of Butyl Acrylate: Effect of Functional Monomers

Chorng-Shyan Chern^a; Feng-Yi Lin^a

^a Department of Chemical Engineering, National Taiwan Institute of Technology Taipei, Taiwan, Republic of China

To cite this Article Chern, Chorng-Shyan and Lin, Feng-Yi(1996) 'Semibatch Emulsion Polymerization of Butyl Acrylate: Effect of Functional Monomers', *Journal of Macromolecular Science, Part A*, 33: 8, 1077 – 1096

To link to this Article: DOI: 10.1080/10601329608010906

URL: <http://dx.doi.org/10.1080/10601329608010906>

PLEASE SCROLL DOWN FOR ARTICLE

Full terms and conditions of use: <http://www.informaworld.com/terms-and-conditions-of-access.pdf>

This article may be used for research, teaching and private study purposes. Any substantial or systematic reproduction, re-distribution, re-selling, loan or sub-licensing, systematic supply or distribution in any form to anyone is expressly forbidden.

The publisher does not give any warranty express or implied or make any representation that the contents will be complete or accurate or up to date. The accuracy of any instructions, formulae and drug doses should be independently verified with primary sources. The publisher shall not be liable for any loss, actions, claims, proceedings, demand or costs or damages whatsoever or howsoever caused arising directly or indirectly in connection with or arising out of the use of this material.

SEMIBATCH EMULSION POLYMERIZATION OF BUTYL ACRYLATE: EFFECT OF FUNCTIONAL MONOMERS

CHORNG-SHYAN CHERN* and FENG-YI LIN

Department of Chemical Engineering
National Taiwan Institute of Technology
Taipei, Taiwan 10672, Republic of China

ABSTRACT

The concentration of sodium lauryl sulfate (SLS) in the initial reactor charge is the most important parameter in determining the latex particle size during semibatch emulsion polymerization of butyl acrylate in the presence of acrylic acid (AA), methacrylic acid, or hydroxyethyl methacrylate. The final latex particle size decreases with increasing concentration of SLS, NP-40, or functional monomer. The carboxylic monomer AA is the most efficient functional monomer to nucleate and then stabilize the latex particles. The plot of $\log N_f$ vs \log SLS shows a slope of 0.4–0.8, which is more consistent with Feeney's analysis based on the coagulative nucleation mechanism. Experimental data also show that the particle size first decreases to a minimum and then increases with an increase in the concentration of the neutralizing agent NaHCO_3 . The optimal concentration NaHCO_3 for achieving the smallest latex particle size occurs at a point close to 0.15–0.29%. Experimental data of the particle size distribution and molecular weight distribution show that the aqueous phase reaction can play a very important role during the particle nucleation period.

INTRODUCTION

Semibatch emulsion polymerization [1–13] is an important process for the manufacture of latex products such as coatings, adhesives, and synthetic elastomers. The semibatch process can easily remove the heat generated during polymerization in addition to its operational flexibility for producing products with controlled polymer composition and morphology. Emulsion polymerization involves the compartmentalized free-radical reaction occurring in a large number of monomer-swollen polymer particles. These polymer particles (ca. 50–1000 nm in diameter) can be dispersed in water by adsorption of anionic surfactants (e.g., sodium lauryl sulfate, SLS) and/or nonionic surfactants (e.g., nonylphenol-40 mole ethylene oxide adduct, NP-40) on the particle–water interface. One drawback associated with conventional surfactants is that the small and mobile surfactant molecules in the latex product can diffuse to the surface layer of the polymeric film and, as a result, the surfactant migration can have a negative effect on such product properties as adhesion of pressure-sensitive adhesives and water resistance of caulks, sealants, and coating materials.

To overcome this problem, the level of surfactants used in the emulsion polymerization process can be reduced. However, the latex stability can be greatly reduced and a significant amount of coagulum can form during the monomer addition period if the latex particles are not adequately protected by the adsorbed surfactant molecules. Removal of the coagulum by filtration is necessary because the filterable solids can have a negative effect on the product properties such as the gloss of the coatings. The reactor needs to be shut down for cleaning when the reactor scrap accumulates to an unacceptable level. Furthermore, the latex particles can grow in size by relatively mild agglomeration in order to maintain appreciable colloidal stability, in addition to polymerizing the imbibed monomer in the particles. The improved latex stability is attributed to the decreased particle surface area and, hence, the increased particle surface charge density associated with such a limited flocculation process [14, 15]. The limited flocculation process can make the task of particle size control more difficult. This is a critical issue since control of the particle size is the key to guaranteeing the quality of the latex products. All these factors will cause significant problems in latex plant production.

The dilemma between satisfactory product properties and smooth plant production places a great challenge in front of polymer chemists. Snuparek [9] and Snuparek and Tutalkova [10] studied semibatch emulsion polymerization of acrylic monomers, and their data showed that incorporation of a small amount of functional monomers such as acrylic acid (AA) into the polymer increased the latex stability significantly. The ionized carboxyl group that is chemically incorporated into the polymer can increase the particle surface charge density and, therefore, increase the repulsive force among the interactive particles. Greene [6, 7] carried out semibatch emulsion copolymerization of styrene, butadiene, and a functional monomer [AA or methacrylic acid (MAA)]. Distribution of the carboxylic monomer unit in the aqueous phase, in the surface layer of the particles, and in the interior of the particles was found to be 2:3:1 and 0.1:1:1 for the latex product incorporated with AA and MAA, respectively. These data suggest that the type of carboxylic monomers should play an important role in the particle nucleation and growth processes. Recently, Chern and Hsu [13] studied semibatch emulsion co-

polymerization of methyl methacrylate (MMA) and butyl acrylate (BA) with the mixed surfactant system SLS/NP-40. It was found that the concentration of SLS in the initial reactor charge was the most important parameter in controlling the final latex particle size. The number of particles formed was proportional to the concentration of SLS in the initial reactor charge to the 0.5–1.2 power and proportional to the concentration of NP-40 in the initial reactor charge to the 0.014–0.72 power. The number of particles was almost independent of the concentration of initiator. Furthermore, the ratio of MMA to BA did not show any significant effect on the particle size. Thus, a simple monomer system containing BA in combination with a small amount of AA, MAA, or hydroxyethyl methacrylate (HEMA) was selected for study because the effect of functional monomers was of primary interest to this work. These kinds of formulations should be useful to the pressure-sensitive adhesive industry. The mixed surfactant system SLS/NP-40, investigated by Chern and Hsu, has been widely used in the commercial production of emulsion polymers. In this work the mixed surfactant system was thus adopted to nucleate and stabilize the latex particles during polymerization.

The objective of this work was to study the effects of important reaction parameters on the particle nucleation and growth processes for semibatch emulsion polymerization of BA in the presence of AA, MAA, or HEMA. The reaction parameters include the concentration of SLS in the initial reactor charge, the concentration of NP-40 in the initial reactor charge, the type and concentration of functional monomers, and the concentration of sodium bicarbonate (a neutralizing agent).

EXPERIMENTAL

Materials

The chemicals used were butyl acrylate (Formosa Plastics Co.), acrylic acid (Formosa Plastics Co.), methacrylic acid (Mitsubishi Rayon), hydroxyethyl methacrylate (Mitsubishi Rayon), sodium lauryl sulfate (Henkel Co.), nonylphenol-40 mole ethylene oxide adduct (Union Carbide), sodium persulfate (Riedel-de Haen), sodium bicarbonate (Riedel-de Haen), sodium hydroxide (Riedel-de Haen), hydrochloric acid (Nacalai Tesque, Inc.), sodium chloride (Riedel-de Haen), hydroquinone (Nacalai Tesque, Inc.), nitrogen (Ching-Feng-Harng Co.), and deionized water (Barnsted, Nanopure Ultrapure Water System, specific conductance $< 0.057 \mu\text{S}/\text{cm}$). The primary monomer BA was distilled under reduced pressure before use. All other chemicals were used as received.

Polymerization Process

Semibatch emulsion polymerization was carried out in a 1-L glass reactor equipped with a 4-bladed agitator, a thermometer, and a condenser. A typical recipe is shown in Table 1, and the polymerization procedure is described below. All process water along with the initial surfactants, sodium bicarbonate, and monomers were charged to the reactor at room temperature. The initial reactor charge was purged with nitrogen for 10 minutes to remove the dissolved oxygen while the reactor temperature was brought to 80°C. The reaction was then initiated by adding

TABLE I. A Typical Recipe of 3×3 Latin Square Design for Semibatch Emulsion Polymerization of BA with a Functional Monomer: (A, a, I, 1)

A I	a 1	B II	a 3	C III	a 2
A II	b 2	B III	b 1	C I	b 3
A III	c 3	B I	c 2	C II	c 1

(A, a, I, 1)	Chemicals	Weight, g
Monomer emulsion feed	H ₂ O	80.00
	SLS	5.67
	BA	205.80
	HEMA	0.20
Initial reactor charge	H ₂ O	450.00
	SLS	0.05
	NP-40	0.05
	NaHCO ₃	0.68
Initial monomer charge	BA	20.92
	HEMA	0.02
Initiator solution	H ₂ O	15.00
	Na ₂ S ₂ O ₈	1.15
Total weight (g)		779.54
Total solids content (%)		30.00

the initiator solution to the reactor. After 15 minutes the monomer emulsion was fed to the reactor over 180 minutes by an FMI pump. The reaction temperature was kept at 80°C throughout the reaction. After the end of the monomer emulsion feed, the reaction system was maintained at 80°C for 30 minutes to reduce the level of residual monomer. The theoretical total solids content at the end of polymerization is 30%.

The latex product was then filtered through a 40-mesh (0.42 mm) screen and a 200-mesh (0.074 mm) screen in series to collect the filterable solids. Scrap adhering to the agitator, thermometer, and reactor wall was also collected. Total solids content was determined by the gravimetric method. The particle size data were obtained from the dynamic light-scattering method (Otsuka, Photal LPA-3000/3100). Molecular weight distribution of the emulsion polymer was determined by gel permeation chromatography (GPC, TSP, Spectra System, P100).

RESULTS AND DISCUSSION

3 × 3 Latin Square Design for Particle Size Control

First, a 3 × 3 Latin square design (4 variables, 3 levels, and 9 experiments, as shown in Table 1) was used to screen the four reaction parameters: the concentration of SLS in the initial reactor charge (A = 0.01%, B = 0.25%, and C = 0.5% based on the weight of water in the initial reactor charge); the type of functional monomers (a = HEMA, b = MAA, and c = AA); the concentration of HEMA, MAA, or AA (I = 0.1%, II = 1%, and III = 10% based on total monomer shown in the recipe); and the concentration of NP-40 in the initial reactor charge (1 = 0.01%, 2 = 0.25%, and 3 = 0.5% based on the weight of water in the initial reactor charge). The remaining parameters were kept constant in this series of experiments: the concentration of initiator and neutralizing agent was 0.25 and 0.15%, respectively, based on the weight of water in the initial reactor charge; the concentration of SLS in the monomer emulsion feed was 2.5% based on total monomer shown in the recipe; and the agitation speed was 400 rpm.

For example, the experiment in the top left corner of the Latin square (A, a, I, 1) consists of 0.01% SLS in the initial reactor charge, 0.1% HEMA, and 0.01% NP-40 in the initial reactor charge, as shown in Table 1. To test the batch-to-batch variations, the experiment (A, a, I, 1) was carried out twice. The average particle size of the finished products was 218 ± 3 nm. Another experiment, the midpoint of the two-level factorial design shown below (recipe: 0.2525% SLS and NP-40 in the initial reactor charge and 5.05% AA), was also carried out twice. In this case the average particle size was 70 ± 1 nm. The reproducibility of both formulas, which result in very different final latex particle sizes, is satisfactory. Please note that the Latin square design does not take into account the interactions among the reaction variables. Therefore, it was used to determine qualitatively the magnitude of the effect of each variable on the properties of the latex product. The experimental data are summarized in Table 2.

The percentage of the particle volume change during the monomer emulsion feed (ΔV , shown in Table 2) can be calculated as follows:

$$\Delta V = [(d_f/d'_f)^3 - 1] \times 100\% \quad (1)$$

where d_f is the measured diameter of the final latex particles. The parameter d'_f is the calculated particle diameter if both secondary nucleation and limited flocculation do not occur during the monomer addition period.

If d_{1s} (nm) and N_p are the diameter and total number of the particles, respectively, of the sample taken immediately before the start of the monomer emulsion feed, W_m (g) is the total weight of the feed monomer, and ρ (g/cm³) is the density of polymer, then d'_f can be calculated according to the following equation:

$$d'_f = [d_{1s}^3 + 6 \times 10^{21} W_m / (\pi \rho N_p)]^{1/3} \quad (2)$$

The numerical value corresponding to the variable (see Table 2) represents the effect of the variable on the latex property. For example, the overall average particle size of the finished products in the Latin square design is 103 nm. The effect of the variables A, B, and C on d_f is +67, -27, and -41 nm, respectively. That is, the

TABLE 2. Effect of Each Reaction Variable on Properties of Latex Product in a 3×3 Latin Square Design^a

	d_{15} , nm	d_f , nm	ΔV , %	40-mesh, %	200-mesh, %
A	42	67	-36	-0.79	-0.0063
B	-18	-27	19	2.06	-0.0024
C	-23	-41	18	-1.27	0.0087
a	5	13	-10	1.63	0.0088
b	1	-2	20	-1.27	-0.0039
c	-6	-11	-10	-0.36	-0.0049
I	7	21	18	0.39	-0.0024
II	3	-2	-7	1.00	-0.0039
III	-10	-19	-11	-1.39	0.0063
1	5	17	74	-0.78	-0.0052
2	3	-6	-32	-0.36	0.0088
3	-9	-10	25	1.14	-0.0036
Overall average	52	103	-7	1.44	0.0095

^a d_{15} : particle size of the latex sampled at the time just before the start of the monomer emulsion feed. d_f : Final latex particle size. ΔV : Percentage of the particle volume change during the monomer emulsion feed. 40-mesh: Scrap collected by a 40-mesh screen plus those adhering to the agitator, thermometer, and reactor wall. 200-mesh: The filterable solids collected by a 200-mesh screen.

experiment containing 0.01, 0.25, or 0.5% SLS in the initial reactor charge (A, B, or C), on the average, can contribute +67, -27, or -41 nm to d_f with respect to the overall average value (103 nm). The greater the range of the numbers (e.g., +67 to -41 nm), the stronger the effect of the variable (e.g., the concentration of SLS in the initial reactor charge) on d_f .

Experimental data show that the concentration of SLS in the initial reactor charge is the major particle generator and it influences d_f the most. On the other hand, NP-40 can impart steric stabilization to the particles, and it acts as an auxiliary emulsifier for promoting the chemical and freeze-thaw stability. The effects of other variables on d_f are of about the same order of magnitude. The parameter d_f decreases with increasing concentration of SLS, NP-40, or functional monomer. At a common concentration of functional monomer, d_f in increasing order is AA < MAA < HEMA. This result indicates that AA is the most efficient functional monomer to nucleate and then stabilize the latex particles. In addition, the overall average data of ΔV , 40-mesh scrap, and 200-mesh filterable solids (see Table 2) show that all of the latices in this series of experiments are relatively stable during polymerization.

Two-Level Factorial Design for Particle Size Control

We then chose the concentration of SLS in the initial reactor charge (0.005–0.5%), the concentration of NP-40 in the initial reactor charge (0.005–0.5%), and the concentration of AA (0.1–10.0%) as the three variables of a two-level factorial design (9 experiments, 1 midpoint included) to analyze quantitatively the effects of these variables on d_f . The two numerical values in parentheses represent the minus level and plus level of that variable in the factorial design. The concentration of SLS in the monomer emulsion feed was 4% based on total monomer instead of 2.5% used in the Latin square design in order to reduce the coagulum formation (see the 40-mesh scrap data in Table 2).

Again, the experimental data show that the concentration of SLS in the initial reactor charge (–42 nm) is the most important parameter in determining d_f . The numerical value in parentheses represents the standardized effect of the variable on d_f when the variable is changed from the minus level to the plus level. The overall average particle size in the factorial design is 98 nm. Based on the factorial design, an equation was derived to predict d_f . Figure 1 shows the contour plot of d_f constructed from the predictive equation. The abscissa is the concentration of NP-40 in the initial reactor charge and the ordinate is the concentration of SLS in the initial reactor charge. In considering the curve with d_f equal to 70 nm, the level of SLS required to maintain the same size remains relatively constant because SLS predominates in the particle nucleation process. On the other hand, the level of SLS required to maintain the same size decreases with increasing concentration of NP-40 for the curves with d_f greater than 90 nm since NP-40 becomes important in this region. Furthermore, the curve for a certain particle size (e.g., 90 nm) shifts toward the bottom left corner when the concentration of AA increases from 0.1 to 10.0%. This trend implies that the levels of both SLS and NP-40 required to maintain the same size drop when a higher concentration of AA is present during polymerization.

Three formulas (L, M, and S) were then selected to verify the predictive equation for d_f . The recipes and experimental data are listed in Table 3. The experimental data agree reasonably well with the predictions. Formula L has the lowest surfactant concentration in the initial reactor charge and, hence, it should have the shortest nucleation time. On the other hand, formula S has the highest surfactant concentration in the initial reactor charge and, hence, the longest nucleation time. Thus, the parameter u/G^2 that reflects the breadth of the particle size distribution in the decreasing order are $S > M > L$ for the 15-minute latex samples, as shown in Table 3. The smaller the value of u/G^2 , the narrower the particle size distribution. In addition, the particle size distribution is monodisperse when $u/G^2 < 0.1$. The particle size distribution data for the final latex samples also show that u/G^2 in the decreasing order are $S > M > L$. All of the particle-size distributions become narrower at the end of polymerization because the residence time distribution for the growing particles becomes narrower as polymerization proceeds.

Figure 2 shows the $\log N_f$ vs \log SLS curves at three concentrations of NP-40 in the initial reactor charge (0.005, 0.25, and 0.5%), where N_f is the final number of particles per liter of water, SLS represents the concentration of SLS in the initial reactor charge, and NP-40 represents the concentration of NP-40 in the initial reactor charge. According to the micellar [16–18] or homogeneous [19–21] nucle-

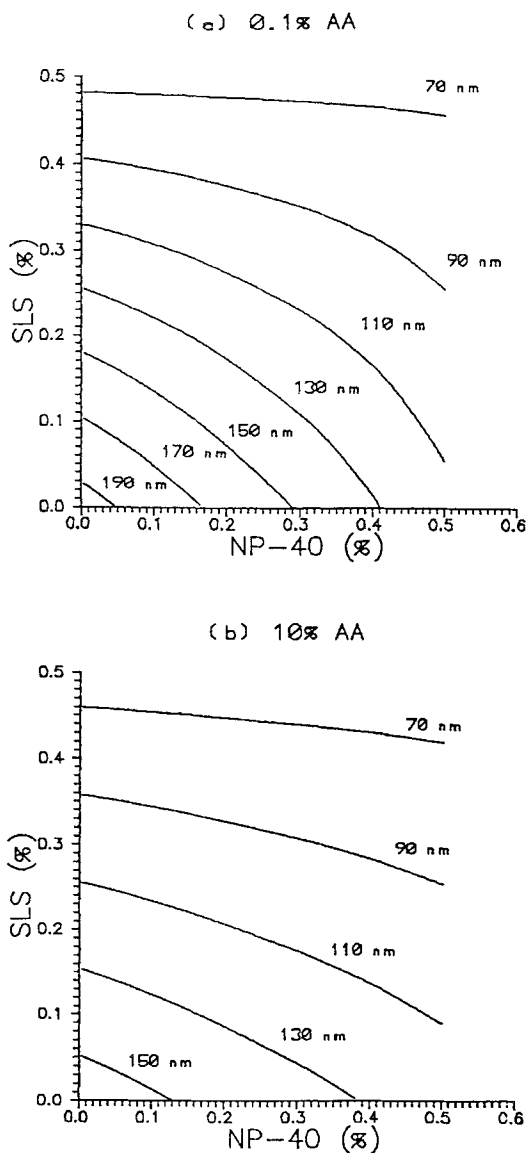


FIG. 1. Contour plot of the final latex particle size.

ation mechanism, the slope of the $\log N_f$ vs \log SLS plot equals 0.6, whereas Feeney et al. [22] showed that the slope of the $\log N_f$ vs \log SLS plot should lie between 0.4 and 1.2 for the coagulative nucleation mechanism. Figure 2 shows that the effect of SLS on N_f strongly depends on the concentration of NP-40 in the initial reactor charge. The slope of the linear portion (a region in which the concentration of SLS is greater than its critical micelle concentration, CMC) of the $\log N_f$ vs \log SLS plot ranges from 0.4 to 0.8, which is more consistent with Feeney's predictions.

TABLE 3. Experiments Designed to Verify Predictive Equation for Final Particle Size

	L	M	S
SLS (%)	0.021	0.168	0.419
NP-40 (%)	0.020	0.200	0.500
AA (%)	0.1	1.0	10.0
Prediction (nm)	190	118	70
Experimental data (nm)	158	96	66
Error (%)	-17	-19	-6
u/G^2 15 minute sample	0.19	0.20	0.31
u/G^2 final sample	0.0003	0.028	0.18

Figure 3 shows the $\log N_f$ vs \log NP-40 plot at four concentrations of SLS (0.005, 0.12, 0.25, and 0.5%). The parameter N_f remains relatively constant with increasing concentration of NP-40 when the concentration of SLS in the initial reactor charge is greater than 0.005% because, as discussed above, SLS plays a predominant role during the particle nucleation period. On the other hand, NP-40 becomes important in determining the number of primary particles generated during the early stage of polymerization when the concentration of SLS is very low (e.g., SLS = 0.005%). Figure 4 shows the $\log N_f$ vs \log AA plot at four concentrations of SLS (0.005, 0.12, 0.25, and 0.5%), where AA represents the concentration of AA. It is shown that the effect of AA on N_f is significant only when concentrations of both SLS and NP-40 in the initial reactor charge are low enough (e.g., SLS = 0.005% and NP-40 = 0.005%).

Chu and coworkers [23, 24] studied the effect of mixed surfactants (anionic and nonionic surfactants) on the acrylic latex particle size and derived the following equation:

$$\begin{aligned} TS_m &= c + d(TS_a + TS_n) \\ &= c + \alpha_a E_a^{b_a} + \alpha_n E_n^{b_n} \end{aligned} \quad (3)$$

where TS is the total particle surface area, E is the amount of surfactant used, and c , d , α_a , α_n , b_a , and b_n are constants. The subscripts m , a , and n represent the mixed, anionic, and nonionic surfactants, respectively. In this work, a nonlinear least-squares best-fit method was used to obtain c , α_a , α_n , b_a , and b_n for the BA/AA system. The calculated parameters along with the data of Chu and coworkers and Chern and Hsu [13] are compiled in Table 4. The parameter α_a is greater than α_n and b_a is greater than b_n , which again supports the conclusion that SLS is more important than is NP-40 in the particle nucleation process. Furthermore, both parameters α_a and α_n (or both b_a and b_n) of the BA/AA system are about two orders of magnitude (or 50–100%) greater than the counterparts of the MMA/BA system, presumably due to the rapidly increased particle surface area (i.e., the decreased particle size) associated with the use of AA.

Fitch and Tsai [15] studied the surfactant-free emulsion polymerization of MMA and isolated oligomers with molecular weights ranging from 256 to 16,800.

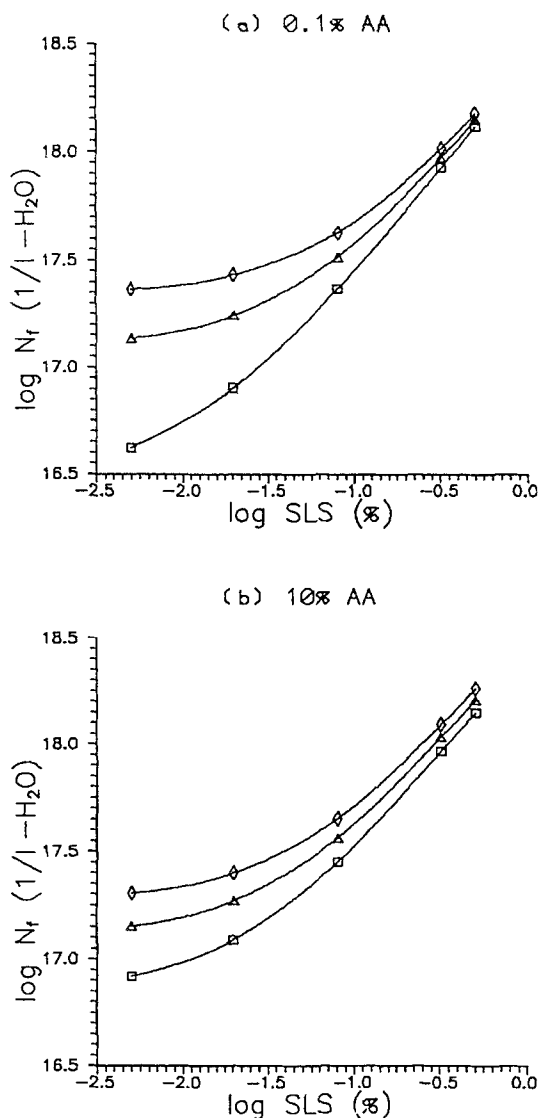


FIG. 2. Number of particles vs concentration of SLS curves: (\diamond) NP-40 = 0.5%; (\triangle) NP-40 = 0.25%; (\square) NP-40 = 0.005%. (a): (\diamond) slope = 0.412; (\triangle) slope = 0.518; (\square) slope = 0.764. (b): (\diamond) slope = 0.489; (\triangle) slope = 0.542; (\square) slope = 0.631.

Goodall et al. [25] studied the surfactant-free emulsion polymerization of styrene and oligomers with a molecular weight of approximate 1000 were also observed during the early stage of polymerization. Figure 5 shows the GPC data for formula L with low concentrations of SLS, NP-40, and AA (0.021% SLS, 0.020% NP-40, 0.1% AA, and $d_f = 158$ nm) at various reaction times. The latex samples taken at different reaction times were short-stopped by hydroquinone. The GPC data clearly

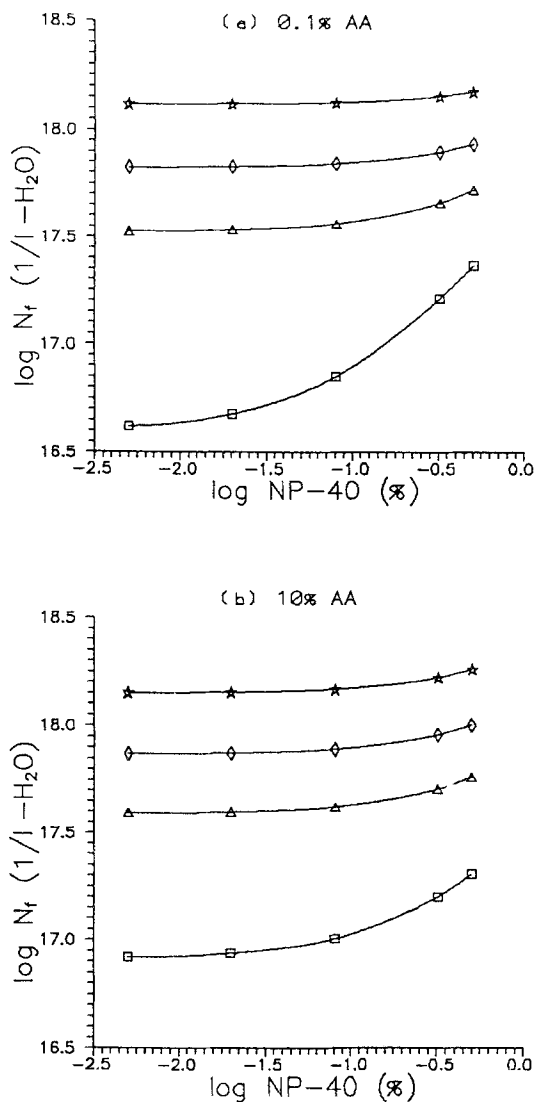


FIG. 3. Number of particles vs concentration of NP-40 curves: (\star) SLS = 0.5%; (\diamond) SLS = 0.25%; (\triangle) SLS = 0.12%; (\square) SLS = 0.005%.

show that low molecular weight oligomers (elution time 24–30 minutes, molecular weight 4000–200) indeed exist during the first 15 minutes of polymerization. The high molecular weight polymer (elution time 15–18 minutes, molecular weight 3.2×10^5 to 7.6×10^4) does exist, but the peak is not significant. Thus, for the polymerization system containing only 0.1% AA, the reaction in the aqueous phase can play an important role during the particle nucleation period. On the other hand, the final latex product shows a strong high molecular weight peak (elution time 12–18 minutes molecular weight 1.4×10^6 to 7.6×10^4), which implies that polymeri-

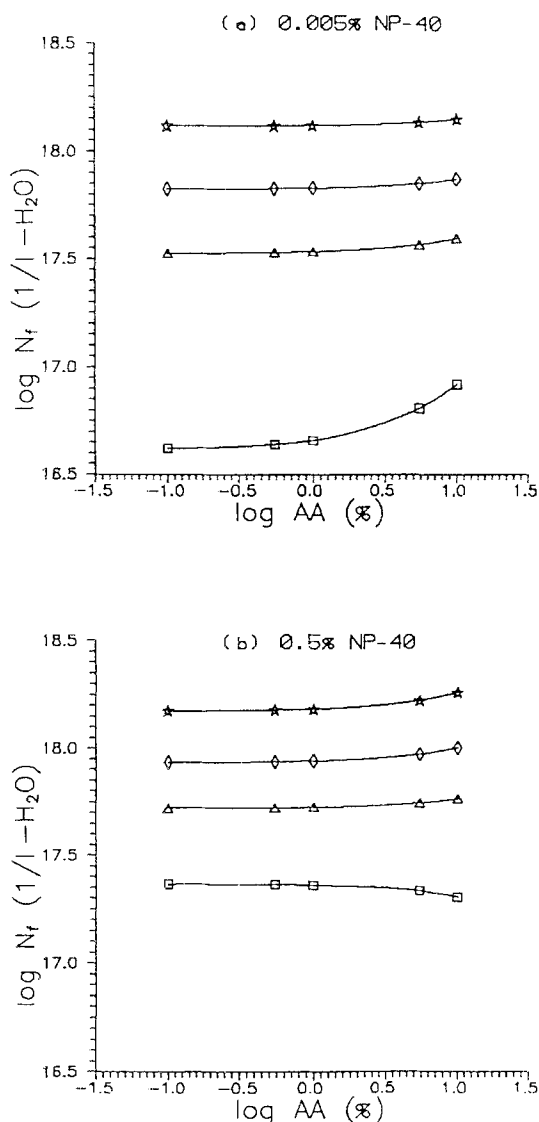


FIG. 4. Number of particles vs concentration of AA curves: (\star) SLS = 0.5%; (\diamond) SLS = 0.25%; (\triangle) SLS = 0.12%; (\square) SLS = 0.005%.

zation in the compartmentalized particles becomes predominant after the particle nucleation process has stopped.

Figure 6 shows the GPC data for the modified formula L (0.021% SLS, 0.020% NP-40, 10% AA, and $d_f = 131 \pm 1$ nm for two identical experiments) at various reaction times. It is interesting to note that the very hydrophilic oligomeric radicals (rich in AA unit) continue to grow to larger molecular sizes, and low molecular weight oligomeric radicals continue to form in the aqueous phase during

TABLE 4. Calculated Parameters to Correlate Total Particle Surface Area to Surfactant Loadings

	c	α_a	b_a	α_n	b_n
MMA (Chu)	2.28×10^{21}	1.15×10^{22}	0.1584	4.94×10^{19}	2.9542
BA (Chu)	-1.75×10^{20}	9.45×10^{20}	0.3180	3.51×10^{20}	0.5560
MMA/BA (50/50) (Chern and Hsu)	5.29×10^{20}	1.19×10^{21}	0.5300	4.76×10^{20}	0.5000
BA/AA	9.00×10^{20}	1.07×10^{23}	1.1000	5.93×10^{22}	0.7800

the first 15 minutes of polymerization. The pattern resembles the tide. In this case a significant amount of polyelectrolyte should have formed during polymerization if the termination and/or chain transfer reactions take place in water or in the particle-water interface. The polyelectrolyte can have an impact on the latex particle size and stability. For example, the polyelectrolyte dissolved in water can compress the electric double layer of the particles and, therefore, reduce the latex stability. On the other hand, the surface-active polyelectrolyte can be adsorbed onto the particle

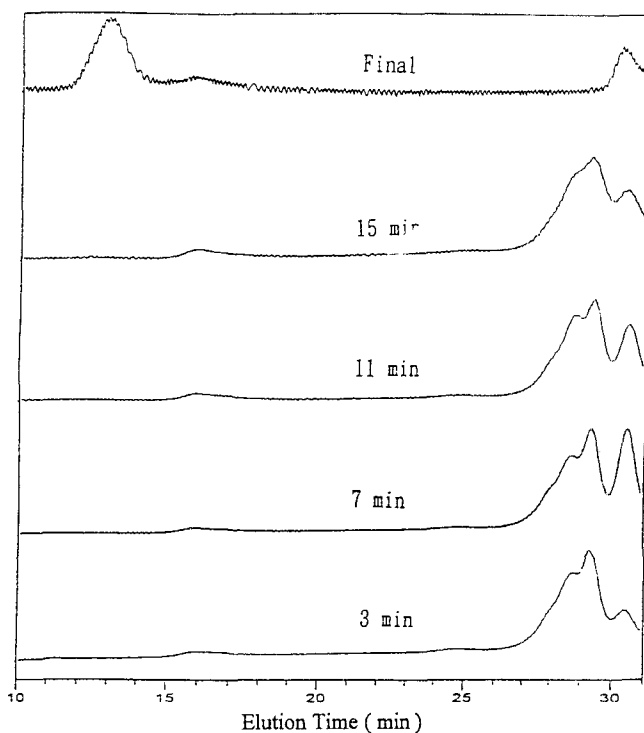


FIG. 5. GPC data of the formula L with low concentrations of SLS, NP-40, and AA (0.021% SLS, 0.020% NP-40, 0.1% AA, $d_f = 158$ nm) at various reaction times.

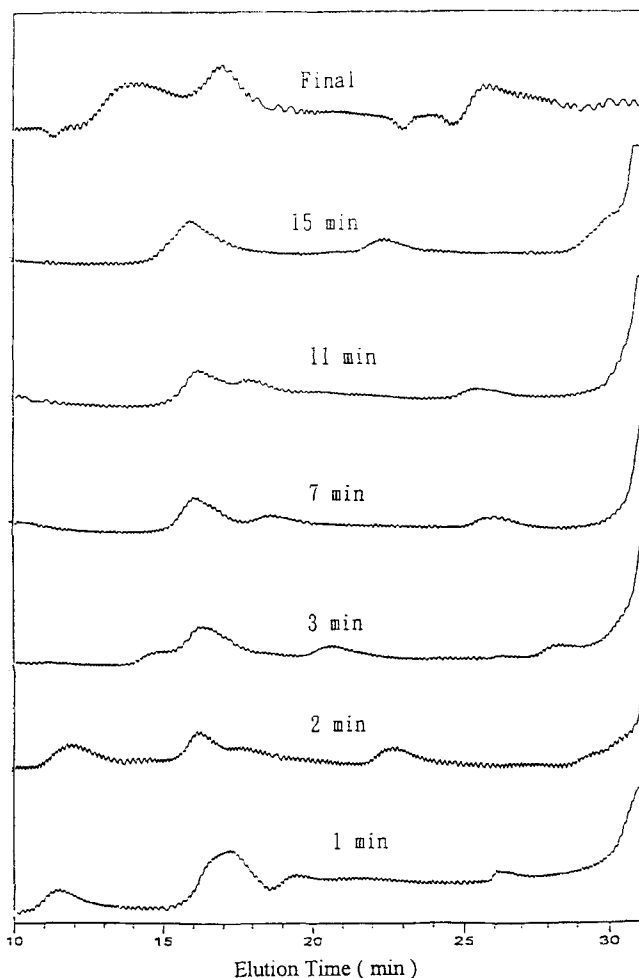


FIG. 6. GPC data of the modified formula L with 10% AA (0.021% SLS, 0.020% NP-40, 10% AA, $d_f = 131$ nm) at various reaction times.

surfaces. The adsorbed polyelectrolyte can increase the particle surface charge density and, consequently, improve the latex stability. A significant quantity of high molecular weight polymer, presumably due to polymerization inside the particles, also exists during the particle nucleation period. This result suggests that AA can help nucleate the primary particles even when the concentration of surfactant is lower than its CMC, which is also supported by the d_f data. That is, the final particle size of the modified formula L with 10% AA (131 nm) is smaller than that of the formula L with 0.1% AA only (158 nm).

Figure 7 shows the GPC data for the formula S (0.419% SLS, 0.500% NP-40, 10% AA, and $d_f = 66$ nm) at various reaction times. The features of the molecular weight distribution of formula S are similar to those of formula L during the first 15 minutes of polymerization except that the peaks at 24–27 and 15–18 minutes

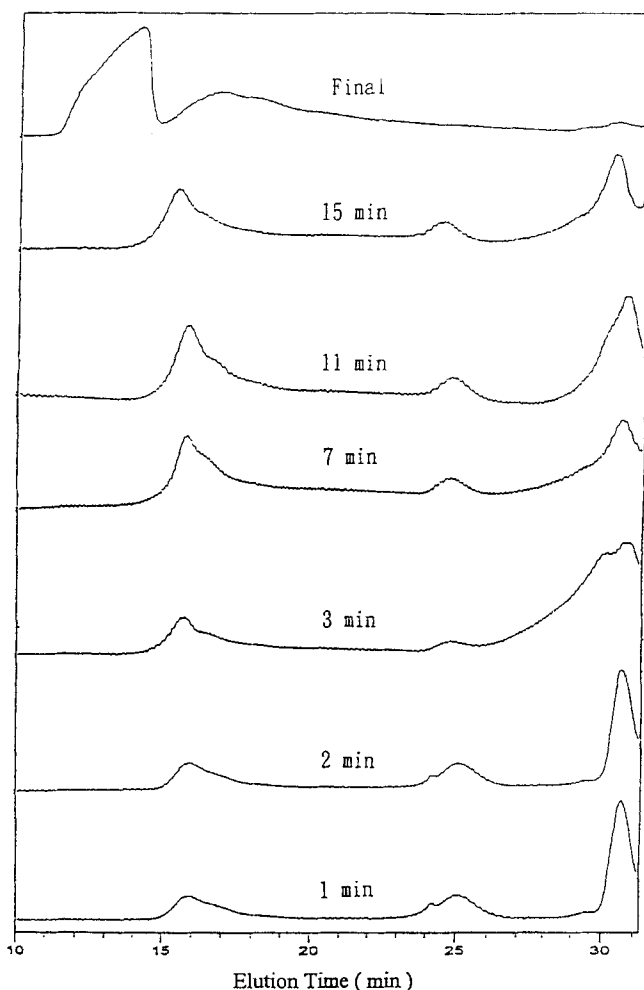


FIG. 7. GPC data of the formula S (0.419% SLS, 0.500% NP-40, 10% AA, $d_f = 66$ nm) at various reaction times.

elution times are quite significant. The peak at 15–18 minutes elution time is attributed to the polymer produced in an extremely large number of latex particles since the concentrations of both SLS and NP-40 in the initial reactor charge are relatively high. On the other hand, the peak at 24–27 minutes elution time is related to the abundant oligomeric radicals generated in the aqueous phase due to the very high concentration of AA. The absence of a tide pattern observed in the modified formula L (see Fig. 6) is probably caused by the rapid absorption of the oligomeric radicals into the growing particles with tremendous particle surface area.

The reagent NaHCO_3 can neutralize the carboxylic group of AA. In this work a series of experiments was used to study the effect of the degree of neutralization of AA on d_f . The concentration of NaHCO_3 was varied from 0 to 0.43% based on the weight of water in the initial reactor charge. Other parameters were kept con-

stant in this series of experiments: the concentrations of the initiator, SLS, and NP-40 were 0.25, 0.01, and 0.01%, respectively, based on the weight of water in the initial reactor charge; the concentration of SLS in the monomer emulsion feed was 4% based on total monomer; the concentration of AA was 5% based on total monomer; the theoretical total solids content was 30% at the end of polymerization; and the agitation speed was 400 rpm. The experimental results are summarized in Table 5.

Table 5 shows that both d_{15} and d_f first decrease to a minimum as the concentration of NaHCO_3 increases from 0 to 0.29% and, thereafter, they increase with increasing concentration of NaHCO_3 . This behavior can be explained by the two counteractive effects: 1) ionization of the carboxyl group to electrostatically stabilize the latex particles and 2) compression of the electric double layer to reduce the latex stability due to the increased ionic strength with the concentration of NaHCO_3 , as predicted by DVLO theory [26, 27]. Another possibility is that at a high concentration of NaHCO_3 (e.g., the concentration of $\text{NaHCO}_3 = 0.43\%$, pH 7.6 at 15 minutes), the fully ionized polyelectrolyte in water can greatly reduce the stability of nucleated particles and, hence, d_{15} increases rapidly (e.g., $d_{15} = 164$ nm). The optimal concentration of NaHCO_3 in the initial reactor charge for achieving the smallest d_f occurs at a point close to 0.15–0.29%.

Novak Model for Particle Nucleation and Growth

Based on the coagulative nucleation mechanism, Novak [11] developed a simple model to describe the particle nucleation and growth processes for the semibatch emulsion polymerization of acrylic monomers:

$$\log d_f = \frac{1}{3} \log(1/G_a) + \frac{1}{3} \log C \quad (4)$$

where G_a is the amount of anionic surfactant used during the particle nucleation period and $C = 6d_{pp}^2 G_f(A_a\rho)$. The parameter d_{pp} is the diameter of the primary particles, G_f is the weight of the final latex particles, and A_a is the particle surface area occupied by a unit weight of the anionic surfactant. In the model development, it was assumed that the precursor particles (ca. 2 nm) were first formed by phase separation of the oligomeric radicals in the aqueous phase. These precursor parti-

TABLE 5. Experiments Designed to Study the Effect of NaHCO_3 Concentration on Final Latex Particle Size

	[NaHCO_3], %			
	0.00	0.15	0.29	0.43
15 minute pH	4.5	5.2	6.8	7.6
d_{15} (nm)	151	134	129	164
Final pH	2.3	3.7	4.1	4.4
d_f (nm)	170	161	156	184

cles, although completely covered with surfactant molecules, were extremely unstable and they aggregated rapidly until a stable (primary) particle size was achieved. The number of primary particles generated during the particle nucleation period was controlled by the amount of surfactant available to stabilize the generated interfacial area. The remainder of polymerization was simply the growth of primary particles via the propagation reaction. There was no flocculation and secondary nucleation occurring during the monomer feed period. The Novak model predicts that the slope of the $\log d_f$ vs $\log(1/G_a)$ plot should be $1/3$, and the intercept can be used to estimate the parameter d_{pp} if the magnitude of the parameter A_a is known.

A series of experiments stabilized with a single anionic surfactant SLS was carried out to study the effect of AA on d_f by means of Novak's model. In this series of experiments the concentration of SLS was varied from 0.01 to 1.00% based on the weight of water in the initial reactor charge. The remaining parameters were kept constant in this series of experiments: the concentration of AA was 5% based on total monomer; the concentrations of initiator and neutralizing agent were 0.25 and 0.15%, respectively, based on the weight of water in the initial reactor charge; the concentration of SLS in the monomer emulsion feed was 2.5% based on total monomer; the theoretical total solids content was 40% at the end of the reaction; and the agitation speed was 400 rpm. For comparison, another series of experiments containing no AA was also carried out in this work. The particle size data are listed in Table 6.

The experimental data are shown in Fig. 8. For the runs containing no AA, the straight line obtained from the least-squares best-fit method has a slope of 0.27, which is lower than the prediction (0.33). This is probably due to secondary nucleation during the monomer emulsion feed. For the runs containing 5% AA the best-fitted straight line has a slope of 0.23. As expected, at a common level of SLS [or $\log(1/G_a)$], the d_f data for the run containing 5% AA is always smaller than that containing 0% AA. However, this trend is less significant as the concentration of SLS in the initial reactor charge increases [or as the parameter $\log(1/G_a)$ decreases]. This is simply because SLS predominates in the particle nucleation process when its concentration is high. It is also interesting to note that the intercept of the straight line is about the same for both series of experiments. The overall average of the parameter d_{pp} was estimated to be 41 nm if the parameters A_a and ρ had values of 0.56 nm^2 [28] and 1 g/cm^3 , respectively. Comparing this value of d_{pp} with the d_{15}

TABLE 6. Experiments Designed to Study the Effect of AA Concentration on Final Particle Size Using Novak's Model

	[SLS], %				
	0.01	0.032	0.100	0.320	1.000
AA = 5%, d_{15} (nm)	103	71	54	40	33
d_f (nm)	174	156	122	91	66
AA = 0%, d_{15} (nm)	115	72	52	38	33
d_f (nm)	223	178	31	94	63

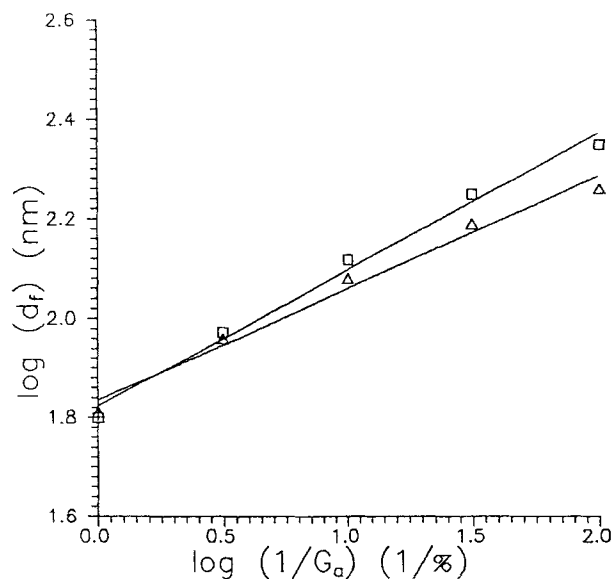


FIG. 8. Final particle size vs reciprocal of SLS level in the initial reactor charge: (\square) AA = 0%; (\triangle) AA = 5%.

data listed in Table 6, the particle nucleation process should stop quickly, and the primary particles will have started to grow to larger sizes long before the start of the monomer emulsion addition when the concentration of SLS in the initial reactor charge is lower than 0.32% ($d_{pp} \ll d_{15}$). This observation corresponds to a shorter particle nucleation time. On the other hand, the particle nucleation process has probably been carried into the monomer emulsion feed period when the concentration of SLS in the initial reactor charge is greater than 0.32% ($d_{pp} > d_{15}$). In this case it corresponds to a longer particle nucleation time. This result is consistent with the particle size distribution data (i.e., the u/G^2 data at 15 minutes) shown in Table 3. Based on the experimental data of the particle size distribution and molecular weight distribution, the semibatch emulsion polymerization of BA with a small amount of AA seems to obey the coagulative nucleation mechanism. However, this statement is not conclusive, and further research on this subject is required to resolve the various particle nucleation mechanisms.

CONCLUSIONS

In the semibatch emulsion polymerization of BA with a small amount of AA, MAA, or HEMA, the concentration of SLS in the initial reactor charge is shown to be the most important parameter for controlling the latex particle size. The concentration of NP-40 in the initial reactor charge is the second most important parameter, and NP-40 acts as an auxiliary stabilizer for promoting the chemical and freeze-thaw stability. The final latex particle size decreases with increasing concentration of SLS, NP-40, or functional monomer. The carboxylic monomer

AA is the most efficient one to nucleate and then stabilize the latex particles among the functional monomers studied. The plot of $\log N_f$ vs $\log SLS$, constructed from the predictive equation based on a factorial design, shows a slope of 0.4–0.8. This result is more consistent with Feeney's analysis based on the coagulative nucleation mechanism. Three formulas (L, M, and S) were selected to verify the validity of the predictive equation, and the experimental data agree reasonably well with the predicted values. Experimental data also show that the particle size first decreases to a minimum and then increases with an increase in the concentration of NaHCO_3 in the initial reactor charge. The optimal concentration of NaHCO_3 for achieving the smallest latex particle size occurs at a point close to 0.15–0.29%.

The Novak model predicts that the slope of the $\log d_f$ vs $\log(1/G_a)$ plot is 0.33 for the coagulative nucleation mechanism. Applying the Novak model to the BA/AA (95/5) system stabilized by a single anionic surfactant SLS results in a slope of 0.23, which is much lower than the prediction. For comparison, another series of experiments containing no AA was carried out and the resultant slope was 0.27. The difference between the slope of the best-fitted straight line for the runs containing 5% AA and that for the runs containing no AA is attributed to the effect of AA. The GPC data for several recipes clearly show that low molecular weight oligomers exist during the first 15 minutes of polymerization. Thus, the aqueous phase reaction can play an important role during the particle nucleation period. On the other hand, the final latex product shows a strong peak associated with the high molecular weight polymer. This result suggests that the propagation reaction taking place in the compartmentalized particles becomes predominant after the particle nucleation process has stopped.

ACKNOWLEDGMENT

Financial support from National Science Council, Taiwan, Republic of China (NSC84-2216-E-011-024) is gratefully acknowledged.

REFERENCES

- [1] P. Fram, G. T. Stewart, and A. J. Szlochtm, *Ind. Eng. Chem.*, **47**, 1000 (1955).
- [2] B. G. Elgood, E. V. Gulbekian, and D. Kinsler, *J. Polym. Sci., B*, **2**, 257 (1964).
- [3] R. A. Wessling, *J. Appl. Polym. Sci.*, **12**, 309 (1968).
- [4] H. Gerrens, *J. Polym. Sci., Part C*, **27**, 77 (1969).
- [5] J. J. Krackeler and H. Naidus, *Ibid.*, **27**, 207 (1969).
- [6] B. W. Greene, *J. Colloid Interface Sci.*, **43**, 449 (1973).
- [7] B. W. Greene, *Ibid.*, **43**, 462 (1973).
- [8] P. Bataille, B. T. Van, and Q. B. Pham, *J. Appl. Polym. Sci.*, **22**, 3145 (1978).
- [9] J. Snuparek Jr., *Ibid.*, **24**, 909 (1979).
- [10] J. Snuparek Jr. and A. Tutalkova, *Ibid.*, **24**, 915 (1979).
- [11] R. W. Novak, *Adv. Org. Coat. Sci. Technol. Ser.*, **10**, 54 (1988).

- [12] B. Li and B. W. Brooks, *Polym. Int.*, **29**, 41 (1992).
- [13] C. S. Chern and H. Hsu, *J. Appl. Polym. Sci.*, **55**, 571 (1995).
- [14] R. M. Fitch, *Br. Polym. J.*, **5**, 467 (1973).
- [15] R. M. Fitch and C. H. Tsai, in *Polymer Colloids* (R. M. Fitch, Ed.), Plenum Press, New York, 1971, pp. 73–116.
- [16] W. D. Harkins, *J. Am. Chem. Soc.*, **69**, 1428 (1947).
- [17] W. V. Smith and R. W. Ewart, *J. Chem. Phys.*, **16**, 592 (1948).
- [18] W. V. Smith, *J. Am. Chem. Soc.*, **70**, 3695 (1948).
- [19] R. M. Fitch, M. B. Prenosil, and K. J. Sprick, *J. Polym. Sci., Part C*, **27**, 95 (1969).
- [20] F. K. Hansen and J. Ugelstad, *J. Polym. Sci., Polym. Chem. Ed.*, **16**, 1953 (1978).
- [21] C. P. Roe, *Ind. Eng. Chem.*, **60**, 20 (1968).
- [22] P. J. Feeney, D. H. Napper, and R. G. Gilbert, *Macromolecules*, **17**, 2520 (1984).
- [23] H. H. Wang and H. H. Chu, *Polym. Bull.*, **24**, 207 (1990).
- [24] H. H. Chu and C. C. Lin, *Ibid.*, **28**, 419 (1992).
- [25] A. R. Goodall, M. C. Wilkinson, and J. Hearn, in *Polymer Colloids II* (R. M. Fitch, Ed.), Plenum Press, New York, 1980, pp. 629–650.
- [26] B. V. Deryagnin and L. D. Landau, *Acta Physicochim. USSR*, **14**, 633 (1941).
- [27] E. J. W. Verwey and J. Th. G. Overbeek, *Theory of the Stability of Lyophobic Colloids*, Elsevier, New York, 1943.
- [28] N. Sutterlin, in *Polymer Colloids II* (R. M. Fitch, Ed.), Plenum Press, New York, 1980, pp. 583–597.

Received September 22, 1995

Revision received November 28, 1995